Ergodic to non-ergodic transition in low concentration Laponite

2004 J. Phys.: Condens. Matter 16 S4993

(http://iopscience.iop.org/0953-8984/16/42/015)

INSTITUTE OF PHYSICS PUBLISHING JOURNAL OF PHYSICS: CONDENSED MATTER

J. Phys.: Condens. Matter **16** (2004) S4993–S5002 PII: S0953-8984(04)79288-7

Ergodic to non-ergodic transition in low concentration Laponite

B Ruzicka, L Zulian and G Ruocco

INFM and Dipartimento di Fisica, Universitá di Roma 'La Sapienza', I-00185 Roma, Italy

E-mail: barbara@systar.phys.uniroma1.it (B Ruzicka)

Received 8 April 2004
Published 8 October 2004
Online at stacks.iop.org/JPhysCM/16/S4993
doi:10.1088/0953-8984/16/42/015

Abstract

At variance with previous determinations, recent investigations on water suspension of a synthetic clay (Laponite) have shown the presence of an arrested phase also at very low clay concentrations (down to $C_w = 0.003$). This surprising behaviour has been studied in a wide clay concentration range. As a result the existence of two different routes towards the arrested phase, applying to low and high Laponite concentrations, has been found. We can speculate that at high clay concentration the system would form a Wigner glass whose elementary units are single Laponite platelets, as already indicated in previous works. At low clay concentrations, in contrast, the Wigner glass is supposed to be composed of clusters of Laponite platelets; in this case the clusters would be stabilized by the competition of long-range electrostatic repulsion and short-range attractive interactions. A similar behaviour has been recently found in a simulation work (Sciortino *et al* 2003 *Preprint* cond-mat/0312161).

1. Introduction

Recent works [2–5] focusing on short-range attractive colloids have opened a new prospective in the field of gel/glass systems, attempting a connection between the gel and the glass arrested state of matter. In these systems, a re-entrant glass line, two kinds of glasses (attractive and repulsive) and a glass–glass line have been predicted [2, 3, 6] and experimentally observed [4, 5]. Correlations between the dynamical behaviour of gels and glasses suggest that a common understanding of these two disordered forms of matter may emerge. A very recent work has investigated the case of further complicated where short-ranged attractive interactions are complemented by weak repulsive electrostatic interactions. In this case the authors have shown that the gel formation process can be fully modelled as a glass transition phenomenon [1]. Despite these recent progresses, a deeper comprehension of the still puzzling liquid–gel transition and of the identity/competition between gel and glass phase as arrested phases in colloidal systems is requested.

In this context the study of Laponite suspension is particularly intriguing because this system has all the characteristics required to investigate this new field of soft matter. Synthetic hectorite clay Laponite is a perfect model for charged platelike colloids. It is in fact composed of nearly monodisperse, rigid, disc-shaped platelets with a well defined thickness of 1 nm, an average diameter of about 30 nm, and a negative surface charge of a few hundred e. In spite of intensive research on Laponite suspensions motivated by its important industrial applications, there is no general agreement about the phase diagram, but it is clear that a very rich phenomenology appears by varying clay concentration and/or ionic strength in the samples. In particular, several arrested phases have been found and there is a very intense discussion about the mechanism that originates these arrested states, attributed by different authors to Wigner glass transition [7, 8], frustrated nematic transition [9–12], micro-segregation [9, 13, 14], gelation [15–17], etc. Long-range electrostatic repulsion and short-range attractive interactions are both present in this colloidal system and the competition between the two interactions makes Laponite suspensions even more interesting. In particular a new phase diagram has shown that we can be in the presence of phase separation, liquid, sol, attractive gel, attractive or repulsive glass, just by changing the clay amount and/or the presence of salt in the solutions [18, 19]. The same authors have also hypothesized a parallelism with the recent works about a reentrant phase indicated before [2–5] and the presence of this phase in the state diagram of Laponite. In this context further studies are necessary to investigate the region where arrested states can be found and their origin.

According to the phase diagram obtained from Mourchid *et al* [9], at ionic strength below $I = 10^{-2}$ M Laponite suspensions can be in two different physical states. Low concentration suspensions ($C_w < C_w^*(I)$) form a stable, equilibrium fluid phase. Higher concentration suspensions ($C_w > C_w^*(I)$) are initially fluids but experience ageing and pass into an arrested phase after a time that depends on the clay amount, as also confirmed by photocorrelation measurements [20, 7, 21–23]. However, recent investigations have shown that the phase diagram needs to be revised. In particular, by dynamic and static light scattering measurements, a surprising arrested phase has been found also at low clay concentrations for very long waiting times [15, 16, 8, 17]. This discovery further complicates the comprehension of Laponite suspensions. Moreover, the understanding of the physical mechanism that can originate an arrested phase at very low clay concentration (at least up to $C_w = 0.3$, see [8]) is particularly intriguing.

In this paper we investigate in detail, by dynamic light scattering, the ageing dynamics and the transition in an arrested phase in two ranges of clay concentrations: in the low and high regions, from 0.3 to 3.1 wt%. Two different aggregation processes for the two regions have been found and a possible explanation for the processes has been proposed.

2. Methods

Laponite is a synthetic hectorite clay manufactured by Laporte Ltd, who kindly supplied us with the material. The powder was firstly dried in an oven at $T = 400$ K for 4 h (up to 20% of the as-received powder weight is due to adsorbed water), then the powder was dispersed in deionized (pH = 7) water, stirred vigorously until the suspensions were cleared and then filtered through 0.45 μm pore size Millipore filters. For some of the samples the pH was measured by a Crison Glp 22 pHmeter; the final value, stable and not dependent on the time elapsed from the filtering, was in the range pH = 9.8–10.0. The suspension was then sealed in a quartz cell. The whole procedure was performed in a glove box under N_2 atmosphere to avoid the observed degradation or dissolution of Laponite particles in the presence of atmospheric CO_2 [24, 25]. The starting ageing time ($t_w = 0$) is defined as the time when the suspension is

filtered. This sample preparation procedure is similar, but not identical, to that already used in previous works [15, 16, 22, 23]. Some authors do not report information on the drying of the powder, others allow the suspension to get in contact with atmosphere, and different details can lead to small differences in the sample behaviour on ageing. In addition, the determination of the sample concentration is also problematic, as the filtering procedure can alter the actual concentration if large clusters are present in the suspension after the stirring phase. To minimize this effect, we prepared a large amount of concentrated solution, then—after filtering—we diluted this parent sample at the desired concentrations. In this way, in the present measurements, the *relative* concentrations are well defined, even if the absolute value in C_w can be affected by a systematic error, that we estimate to be in the range $\Delta C_w/C_w \approx 0.1$.

Dynamic light scattering measurements were performed using an ALV-5000 logarithmic correlator in combination with a standard optical set-up based on an He–Ne ($\lambda = 632.8$ nm) 10 mW laser and a photomultiplier detector. The intensity correlation function was directly obtained as $g_2(q,t) = \langle I(q,t)I(q,0)\rangle/\langle I(q,0)\rangle^2$, where q is the modulus of the scattering wavevector defined as $q = (4\pi n/\lambda)\sin(\theta/2)$ ($\theta = 90^\circ$ in the present experiment). For the low concentration samples ($C_w < 1.8\%$) the measurements were repeated once a week for a long period of time (up to four months for the lowest concentration), while for $C_w > 1.8\%$ the sample was left in the scattering system and photocorrelation spectra were continuously acquired until gelation was reached.

3. Results

Correlation functions at increasing waiting times t_w for two different samples at low (figure 1(A)—$C_w = 1.1$ wt% $< C_w^*$) and high concentration (figure 1(B) $C_w = 2.5$ wt% $> C_w^*$) are reported in figure 1. It is evident from the figure that both the samples are actually performing ageing: also in the case of $C_w = 1.1\%$ the dynamics becomes slower and slower for increasing waiting time t_w. The ageing was unexpected for the lower concentration sample, where a stable liquid state was predicted from the phase diagram [9]. On the contrary, it is evident from figure 1(A) that the system is ageing and that for the longest waiting time reported ($t_w = 2640$ h) a crossover from a complete to an incomplete decay of the correlation function is found. This behaviour is the indication of an ergodicity breaking, a signature of a transition towards an arrested state. Our dynamic light scattering measurements showed that for all the samples studied, down to the lowest concentrated one ($C_w = 0.3$ wt%), there is a typical waiting time, t_w^∞, increasing with decreasing clay concentration C_w, at which the system undergoes an arrested state [8]. With decreasing Laponite concentration this waiting time can vary from hours to several months.

The correlation functions (figure 1) decay following a two step behaviour; this indicates that two different relaxation processes, a fast and a slow one, are present in the system. In order to describe the two processes quantitatively $g_2(q,t) - 1$ has been fitted [22] by the squared sum of two contributions. While the long term contribution is manifestly non-Debye, the short term one can be fitted using a single exponential decay, and no statistical need is found for its stretching.

$$g_2(q,t) - 1 = b(a\mathrm{e}^{(-t/\tau_1)} + (1-a)\mathrm{e}^{(-(t/\tau_2)^\beta)})^2. \tag{1}$$

Here b represents the coherence factor and a, τ_1, τ_2 and β are shape fitting parameters. The fits are shown as full curves in figure 1, and equation (1) describes well the photocorrelation spectra for all the ageing times in the liquid (ergodic) phase for all the measured concentrations.

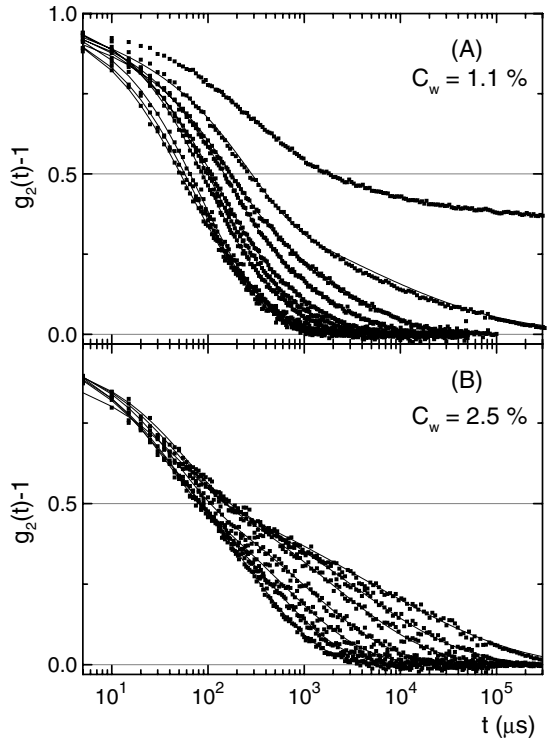

Figure 1. Evolution of the measured intensity correlation functions (symbols) and corresponding fits with equation (1) (continuous lines) for two different Laponite suspensions at the indicated concentrations at different waiting times t_w. The curves are measured at increasing waiting times (from left to right) $t_w = 288, 792, 1128, 1464, 1632, 1800, 1968, 2136, 2328, 2640$ h for sample (A) and $t_w = 6, 30, 54, 78, 102, 126, 150$ h for sample (B) (for which only data in the ergodic phase are reported).

The dynamic structure factor can be directly obtained by inverting the Siegert relation:

$$f(q,t) = \sqrt{\frac{g_2(q,t)-1}{b}}. \tag{2}$$

As an example the dynamic structure factor (open circles) for the sample at $C_w = 1.1\%$ at $t_w = 2328$ h, the fit (full curve) and the two contributions (dotted and dashed curves) are reported in figure 2. From this figure the goodness of fit is evident, and one can also easily identify how the two different terms of equation (1) contribute to the fit. The fast decay (dotted curve of figure 2), characterized by the correlation time τ_1, is well described by the simple exponential term in equation (1), while the slow decay (dashed curve of figure 2), characterized by the correlation time τ_2 and the stretching exponent β, is well described by the stretched exponential part of equation (1).

One important peculiarity of the correlation functions is that the ageing process evolves differently for the lower and higher concentration samples. This is clearly evident directly from the raw measurements reported respectively in figures 1(A) and in (B). For the higher concentration sample (figure 1(B)) the first decay of the correlation function, characterized by the fast process and so by the correlation time τ_1, remains essentially constant, while the second decay, characterized by the slow process and so by the correlation time τ_2, is increasing

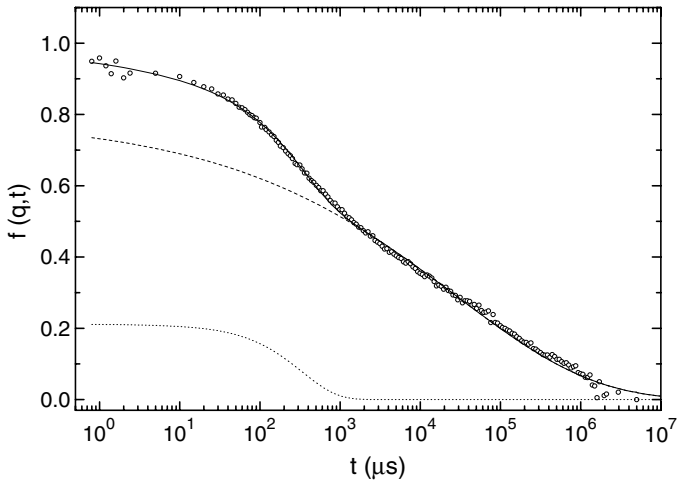

Figure 2. Dynamic structure factor $f(q,t)$ (open circles) of the sample at $C_w = 1.1\%$ at waiting time $t_w = 2328$ h and corresponding fit with equation (1) (full curve). The two contributions of the fit are also reported as the dotted curve for the simple exponential term and the dashed curve for the stretched exponential one.

more and more with ageing. In contrast, for the lower concentration sample (figure 1(A)) all the curve, both the first and the second decays, is increasing with waiting time, so both the relaxation times, τ_1 and τ_2, are increasing with ageing. This is confirmed from the results of the fits, which also shows another major difference between the samples at low and high concentrations as we will show later in the paper.

Now we will focus our attention on the dependence of the parameters obtained from the fit on waiting time t_w and on clay concentration C_w. First we show the behaviour of the parameters of the slow decay: the relaxation time τ_2, the stretching exponent β and the 'mean' relaxation time τ_m of the stretched exponential. If $f(\tau')$ is the distribution function of relaxation times that gives rise to a stretched decay

$$e^{-(t/\tau_2)^\beta} = \int_0^\tau f_{\tau_2,\beta}(\tau') e^{-t/\tau'} \, d\tau' \tag{3}$$

then the mean relaxation time is defined as

$$\tau_m = \int_0^\tau \tau' f_{\tau_2,\beta}(\tau') \, d\tau' \tag{4}$$

and it results to be

$$\tau_m = \tau_2 \frac{1}{\beta} \Gamma\left(\frac{1}{\beta}\right). \tag{5}$$

As an example, the values of τ_2 and τ_m in the function of waiting times t_w obtained for three different concentrations are reported in figures 3(A) and (B), respectively. It is evident that the mean relaxation time τ_m is larger than τ_2 and it spans more decades, but the behaviour of the two relaxation times is the same: both τ_2 and τ_m seem to diverge at a given waiting time t_w^∞, i.e. when the system is arrested. This clearly shows that the samples at low concentrations are also actually ageing and undergo a transition in an arrested phase. It is evident from figure 3 that the dependence of both τ_2 and τ_m on t_w is faster than exponential. To have more

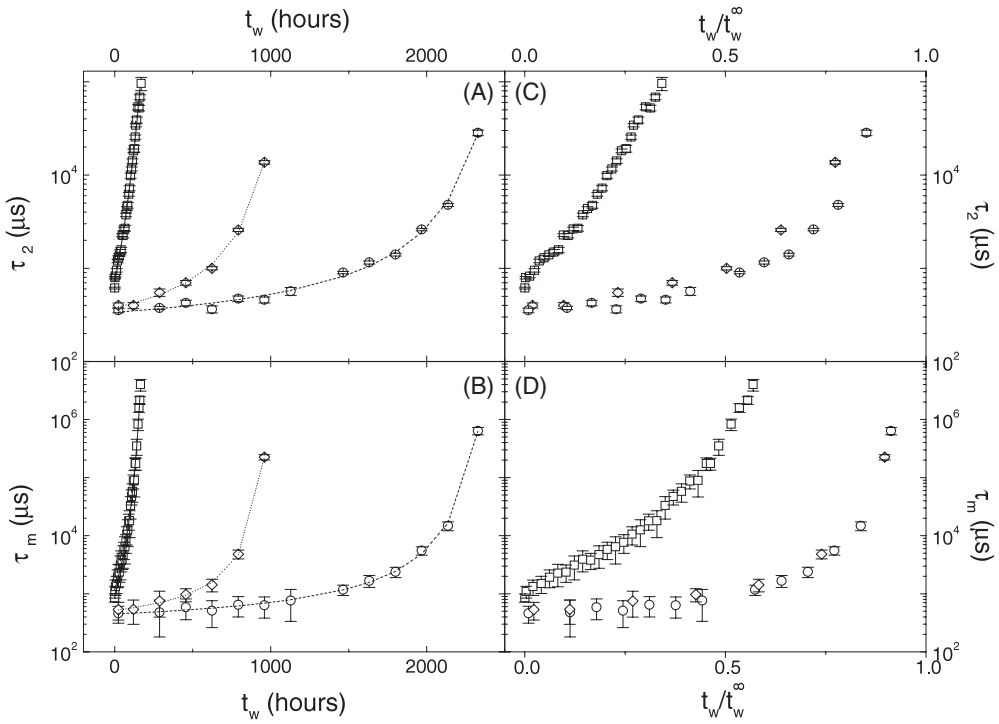

Figure 3. Waiting time dependence for three concentrations (C_w: ○ = 1.1%; ◇ = 1.5%; □ = 2.5%) of τ_2 (panel A) and of τ_m (panel B) extracted respectively from the fit analysis (equation (1)) and from equation (5). Continuous curves are fits of τ_2 with equation (6) (panel A) and of τ_m with equation (7) (panel B). The same relaxation times τ_2 and τ_m are respectively reported in the function of t_w/t_w^∞ in panel C and in panel D.

information about the aggregation process we represent the ageing time (t_w) dependence of the relaxation times as

$$\tau_2 = \tau_2^0 \exp\left(A\frac{t_w}{t_w^\infty - t_w}\right) \tag{6}$$

and

$$\tau_m = \tau_m^0 \exp\left(B\frac{t_w}{t_w^\infty - t_w}\right). \tag{7}$$

The expressions (6) and (7) can be considered a generalization to long waiting time of the exponential growth of τ_2 with t_w observed by Abou *et al* [22] in high concentration samples. Equation (6)—reported in figure 3(A) as full curves—and equation (7)—reported in figure 3(B) as full curves—describe the measurements well. The same quantities, τ_2 and τ_m, are reported in figures 3(C) and (D), respectively, as a function of the waiting times renormalized as t_w/t_w^∞, where t_w^∞ is obtained from the fit analysis described by equations (6) and (7). As is evident from these panels, also in this case both relaxation times, τ_2 and τ_m, have the same behaviour: we observe a collapse of the two data at low concentrations ($C_w = 1.1\%$ and 1.5%). In the remainder of the paper we will focus our attention on the behaviour of the mean relaxation time τ_m.

The most significative parameter of the fits, B, for all the studied concentrations is shown in figure 4. Here the vertical dotted line indicates the concentration that, in the phase diagram [9],

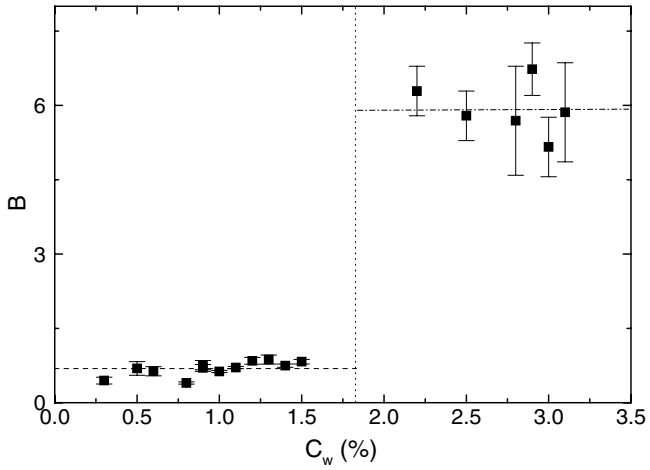

Figure 4. Concentration dependence of the parameter B in equation (7). The dashed lines are guides to the eyes.

would mark the transition from the 'liquid' to the gel phase at $I = 10^{-4}$. The results of the fit indicate that the parameter B, which measures how fast τ_m approaches divergence, is almost constant for all the samples in the low concentration region, while it shows a large discontinuity on passing through the higher concentration region. It is important to note that this jump takes place in a region that encompasses the supposed 'liquid–gel transition' line.

The fact that the value of the B parameter is constant for all the low concentration samples is an indication of the existence of a scaling law. Indeed, if we plot the quantities τ_m and β as a function of t_w/t_w^∞ all the different C_w data with constant B should collapse on a single master curve. The τ_m and the β parameters as a function of the normalized waiting time are reported in figures 5(A) and (B), respectively. As expected, all the data for both the τ_m and the β parameters of lower concentrations collapse, within their statistical uncertainties, on a single curve, while the data at higher clay concentrations have a different behaviour. We already observed from the direct comparison of figures 1(A) with (B) that the ageing process is qualitatively different for the low and high concentration samples. Figures 4 and 5 quantify this difference in the physical properties characterizing the ageing phenomenon in the two different concentration regions.

In figure 6 the behaviour of the fast relaxation time, τ_1, as a function of the same quantity, t_w/t_w^∞, for some of the concentrations studied is reported. A comparison between this figure and figure 5 permits us to make some important observations. As is evident from figure 6, the shorter of the two relaxation times τ_1 does not scale as the mean relaxation time τ_m of the slow process did; in fact the data at $C_w < 1.8\%$ (open symbols) do not collapse on a single master curve as was the case in figure 5 for τ_m. This means that the two relaxation times are really describing two different decay processes and that the factorization of equation (1) into two terms (the exponential one and the stretched exponential one) with two different relaxation times is really necessary. The second important observation regards the different behaviour of the fast relaxation time for low and high concentration samples. The low concentration samples (open symbols in figure 6) show an increase of τ_1 with increasing t_w/t_w^∞, and this is stronger as the Laponite concentration is decreased. On going for example from $C_w = 1.5\%$ (open down triangle) to $C_w = 0.3\%$ (open circle dot centred—lowest concentration measured) the relaxation time τ_1 is more and more increased at increasing waiting time. In contrast, the

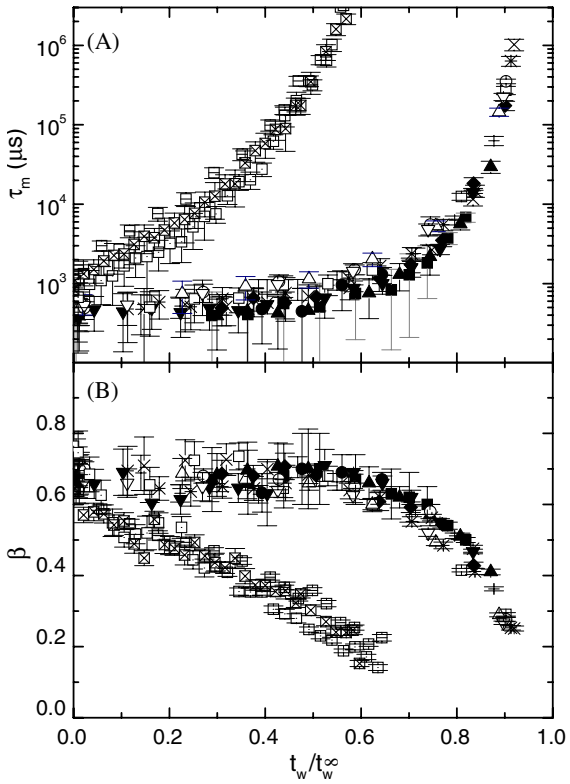

Figure 5. The waiting time dependence of τ_m (A) and β (B) are reported as a function of the scaled variable t_w/t_w^∞ for some of the investigated concentrations: ■ = 0.3%, ● = 0.5%, ▲ = 0.6%, ▼ = 0.8%, ♦ = 0.9%, + = 0.9%, × = 1.0%, ∗ = 1.1%, □ = 1.2%, ○ = 1.3%, △ = 1.4%, ▽ = 1.5%, ⊡ = 2.2%, ⊠ = 2.5%, ⊟ = 2.8%. The data for $C_w < 1.8\%$ collapse on a single master curve.

high concentration samples (full symbols) are essentially constant in all the ergodic (liquid) phase. This analysis of the fit parameter τ_1 confirms our previous observation made directly on the raw data of figure 1.

4. Conclusions

In conclusion the present observations indicate that the aggregation process for the samples at $C_w < C_w^*$ and those at $C_w > C_w^*$ is basically different. This is evident from the behaviour of τ_m and β reported in figure 5 and from the discontinuity of the B parameter across the $C_w = C_w^*$ line as shown in figure 4.

We can speculate about the origin of these different aggregation processes. The microscopic interaction between Laponite platelets is due to a screened Coulomb interaction that can be modelled by a Yukawa-like repulsion at long distances and a quadrupolar electric term at short distances [26, 27]. The competition of short-range attraction and long-range repulsion determines the complexity of the state diagram and of several aggregation processes found changing the ionic strength I and/or the concentration of Laponite. Flocculation, liquid, gel and glassy phases are in fact found in the Laponite phase diagram as also proposed in a recent papers [18, 19], where however the phase at low clay concentration should be also in

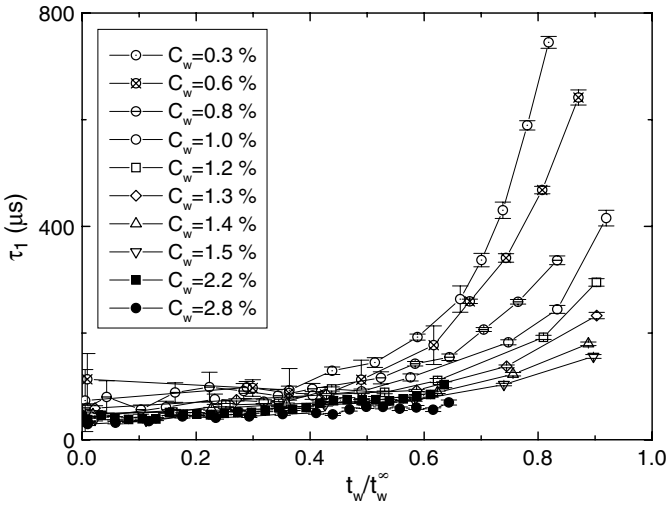

Figure 6. The waiting time dependence of τ_1 is reported as a function of the scaled variable t_w/t_w^∞ for the concentrations indicated in the figure. The data for $C_w < 1.8\%$ do not collapse on a single master curve.

an arrested phase, not in a liquid phase. In particular the presence of long-range repulsion and short-range attraction interactions resembles that recently proposed [1] to describe the phenomenology of colloidal gels. In [1] it has been suggested that the gelation taking place in attractive colloidal suspensions at very low concentration involves the growth of larger and larger clusters (driven by the short-range attraction). The cluster–cluster interaction is essentially controlled by the Yukawa repulsion, due to the short-range nature of the attractive part of the potential. Simulation results show that the cluster ground state shows a minimum at a finite size N^*, indicating that clusters of size larger than N^* are energetically disfavoured. The gel formation process can be fully modelled as a glass transition phenomenon where these clusters are trapped in repulsive cages generated by the long-range repulsions, providing a unifying description of colloidal gels in terms of Wigner glass. We can hypothesize that—at low concentrations—the long time needed to form the arrested phase is spent by the systems in building up the clusters, and that low concentration Laponite suspensions behave as the attractive colloids in [1]. In this view the arrested phases in the low and high clay concentration regions can be viewed as being due to the formation of a Wigner glass. The difference in the two processes would be that at low concentrations the Wigner glass is composed of clusters while at high concentrations, where the packing fraction of the Debye–Huckel sphere associated with each plate reaches value as high as 0.43 [7], the single Laponite platelets would be the elementary constituent of the Wigner glass. This speculation also finds some support in the different behaviour of the relaxation time τ_1 of the fast dynamics analysed previously. While in fact (see figure 6) at high concentrations τ_1 remains essentially constant during the ageing process toward the arrested phase, in the samples at low concentrations it increases with waiting time, probably indicating the formation of clusters of larger and larger dimensions.

References

[1] Sciortino F, Mossa S, Zaccarelli E and Tartaglia P 2003 *Preprint* cond-mat/0312161
[2] Bergenholtz J and Fuchs M 1999 *Phys. Rev.* E **59** 5706
[3] Fabbian L *et al* 1999 *Phys. Rev.* E **59** R1347

[4] Pham K N *et al* 2002 *Science* **296** 104
[5] Eckert T and Bartsch E 2002 *Phys. Rev. Lett.* **89** 125701
[6] Zaccarelli E *et al* 2002 *Phys. Rev.* E **66** 41402
[7] Bonn D *et al* 1998 *Europhys. Lett.* **45** 52
[8] Ruzicka B, Zulian L and Ruocco G 2004 *Preprint* cond-mat/0402157
[9] Mourchid A *et al* 1995 *Langmuir* **11** 1942
[10] Kroon M, Vos W L and Wegdam G H 1998 *Phys. Rev.* E **57** 1962
[11] Gabriel J C P, Sanchez C and Davidson P 1996 *J. Phys. Chem.* **100** 11139
[12] Mourchid A *et al* 1998 *Langmuir* **14** 4718
[13] Pignon F *et al* 1997 *Phys. Rev.* E **56** 3281
[14] Martin C *et al* 2002 *Phys. Rev.* E **66** 21401
[15] Nicolai T and Cocard S 2001 *J. Colloid Interface Sci.* **244** 51
[16] Nicolai T and Cocard S 2001 *Eur. Phys. J.* E **5** 221
[17] Mongondry P, Tassin J F and Nicolai T *Preprint*
[18] Tanaka H, Meunier J and Bonn D 2004 *Phys. Rev.* E **69** 31404
[19] Tanaka H, Meunier J and Bonn D 2004 *Phys. Rev.* E submitted
[20] Kroon M, Wegdam G H and Sprik R 1996 *Phys. Rev.* E **54** 6541
[21] Knaebel A *et al* 2000 *Europhys. Lett.* **52** 73
[22] Abou B, Bonn D and Meunier J 2001 *Phys. Rev.* E **64** 021510
[23] Bellour M *et al* 2003 *Phys. Rev.* E **67** 031405
[24] Thompson D W and Butterworth J T 1991 *J. Colloid Interface Sci.* **151** 236
[25] Mourchid A and Levitz P 1998 *Phys. Rev.* E **57** R4887
[26] Dijkstra M, Hansen J P and Madden P A 1995 *Phys. Rev. Lett.* **75** 2236
[27] Trizac E *et al* 2002 *J. Phys.: Condens. Matter* **14** 9339